

**TEAM2024-00024**

## **CLAMPING TOOLS PRINTED FROM ONYX AND USED IN INDUSTRIAL MANUFACTURING PROCESS**

Michal Prusa<sup>1</sup>, Petr Nemecek<sup>1</sup>, Jiri Hajnys<sup>1</sup>, Jakub Mesicek<sup>1</sup>, Antonin Trefil<sup>1</sup>, Marek Pagac<sup>1</sup>, Jana Petru<sup>1</sup>, Robert Cep<sup>1</sup>

<sup>1</sup>Department of Machining Assembly and Engineering Metrology, Faculty of Mechanical Engineering, VSB -Technical University of Ostrava, 70800 Ostrava, Czech Republic.

### **Abstract**

The publication verifies the theoretical possibilities of reducing production costs and production time for machine clamping jaws. The primary idea involves maintaining the design for conventional production while replacing the steel alloy 1.7225 with the ONYX plastic composite material reinforced with carbon fiber. The study was first verified computationally and then experimentally in industrial operations. The results of the study were recorded and carefully analyzed. The usability of the ONYX composite, in conjunction with carbon fiber, does not support its use in industrial operations. Although the rotary system was significantly lighter, the clamping elements exhibited relatively high elasticity values. Therefore, the results were unsatisfactory but highly beneficial for the practice and usability of plastic composites.

### **Keywords:**

additive manufacturing, clamps, 3D print, plastic, Markforged, clamp printed, machining, turning, composite, carbon

## **1 INTRODUCTION**

To maximize the potential of 3D printing, it is crucial to adapt the design of the entire model and, consequently, the printout as much as possible. Topological optimization [1] is one way to get the most out of 3D printing. Among other benefits, topological optimization [2] can help reduce weight and manufacturing costs [3], provided that the strength and functionality of the part or assembly are maintained. The combination of 3D printing with topological optimization is increasingly used mainly in the aviation industry [4], cosmonautics, and, last but not least, the healthcare sector. The potential of 3D printing in the healthcare sector is still in its infancy. This includes not only bone substitutes or various joints [5], which, thanks to their structure [6], can grow through human tissue and thus perfectly connect inorganic matter with organic matter [7]. Alternatively, it serves as a supportive measure that ensures further organic cell growth [8]. The technology also has applications in orthodontics [9].

3D printing technology is not only applied in advanced and cutting-edge fields but is increasingly seeping into everyday life, for example, in the form of 3D printing of houses [10], apartments, and other residential and non-residential spaces [11]. The advantages include greater speed, less demanding processes, and reduced financial costs [12], which are constantly decreasing with more widespread adoption [13]. For example, printed forms or their parts are already used in industry today, primarily due to the possibility of incorporating precise cooling channels, which

allow controlled cooling of the molds. This not only increases their service life but also improves the quality of the casting. Among other proven technologies is the 3D printing of sand forms, which is notable for its speed of production and subsequent casting, especially of cast iron castings [14]. In these cases, there is no need for special models, making this technology more profitable for small-scale or prototype production.

Today, metal materials are already commonly used in industry, but they are financially very expensive, so significant savings cannot currently be achieved. On the other hand, plastic materials and their composites [15] represent a promising future [16], which, however, has yet to be fully realized and developed. The development of composite materials is ongoing, and further combinations of materials and their mechanical and electrical properties can be expected [17].

In this article, however, the primary focus is on the 3D printing of plastic composites and their use in an industrial environment. The basic material is ONYX [18] and composite carbon fibers [19]. The main idea is to use high-strength composite plastic material, with the best testing conducted in a demanding industrial environment [20]. In this study, the test element is a clamping jaw, which must withstand relatively large clamping pressures and high rotations. If the idea proves successful in practice, its applications could be extensive, not only in clamping technology but also in other sectors such as preparation equipment, clamping blocks, and others.

## 2 MATERIALS AND METHODS

### 2.1 Definition of basic selection conditions

#### 2.1.1 Selection of clamping jaws

Based on the accumulated experience with external clamps, it became clear that the priority is to choose the right shape of the clamp. This shape should withstand high clamping and machining pressures, and its design, in conjunction with the correct laying of composite fibers, should endure a high number of machining cycles without causing permanent deformation. The maximum dimensions of the clamp are 65.9 x 95 x 35 mm. Clamps are originally made of steel 1.7225 (marked according to EN - 42CrMo4). In this experiment, the clamps were made of ONYX material with carbon fiber. The weight of one plastic clamp is 72.6 g.

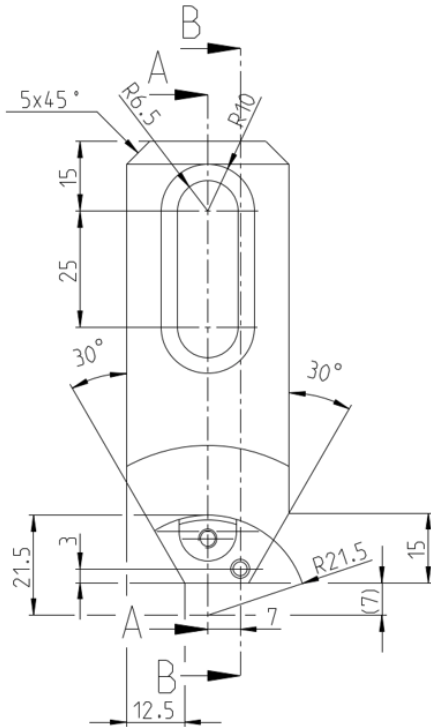


Fig. 1: Sketch of the internal clamp - top view.

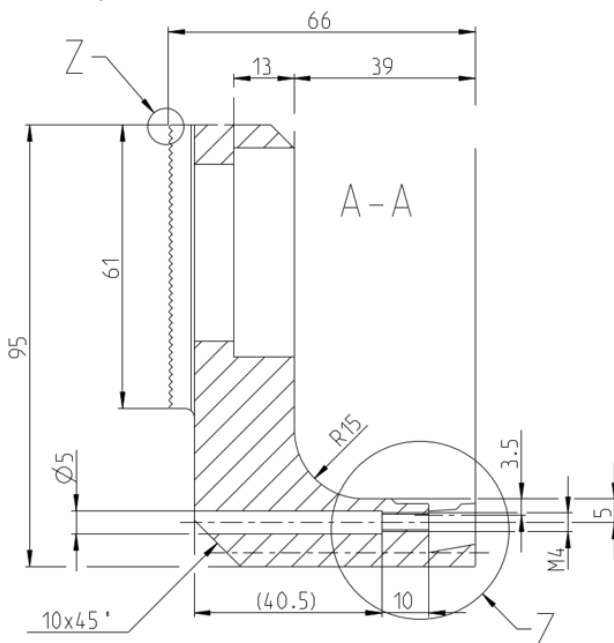


Fig. 2: Sketch of the internal clamp - section from the left side.

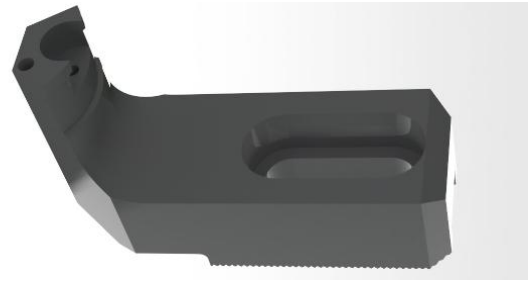


Fig. 3: 3D model of internal clamp.

The assembly of clamps together with the machined part then looks as follows:

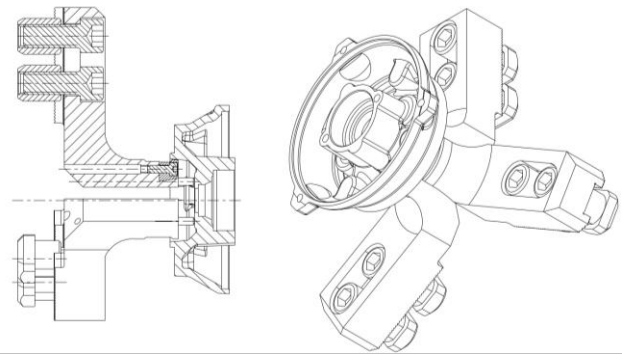


Fig. 4: Sketch of the assembly of an internal clamp with a clamped workpiece.

#### 2.1.2 Selection of the appropriate chuck and associated machine tool

Due to the nature of the clamping of the clamps and the dimensions of the teeth of the clamping part, a chuck from the company Forkardt Deutschland was used and it was a type 3QLC 200 Z6.

This type of chuck was subsequently implemented on the EMAG VL5 machine tool.

#### 2.1.3 Selecting the type of machined part

The type of machined material is already derived from the clamps in parallel. In this case, it was an electric motor end-shield made of EN AC-AISi7Mg0.3 with a diameter of 94 mm and a weight of 140 g.



Fig. 5, 6: Machined part of the electric motor - "end-shield".

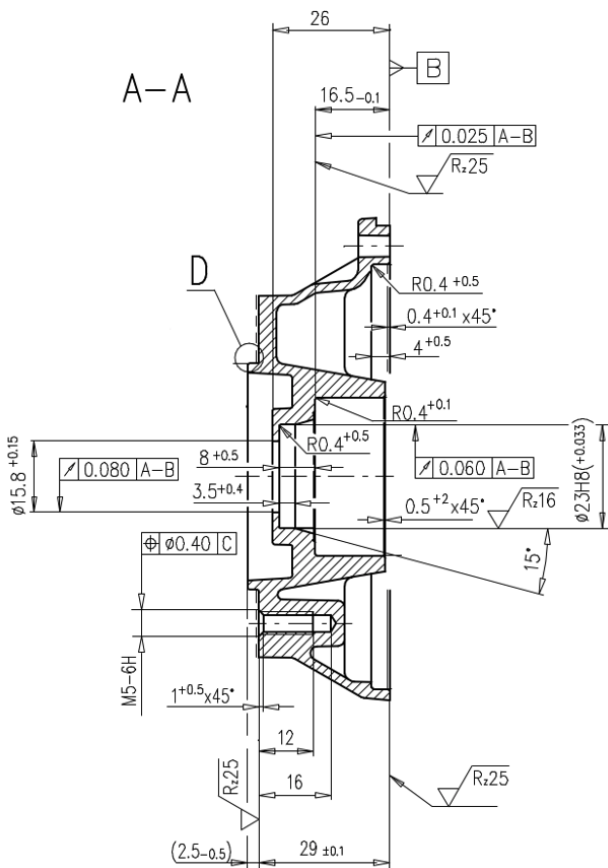


Fig. 7: Sketch of the machine part – cut in plate.

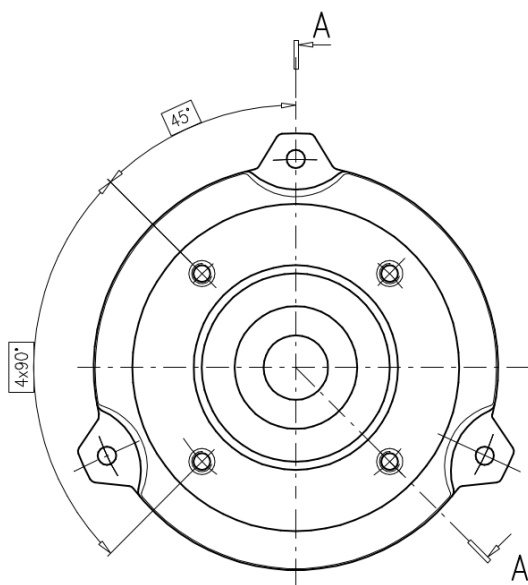


Fig. 8: Sketch of the machine part - top view.

## 2.2 Definition of advanced selection conditions

### 2.2.1 Selection of 3D printing technology to produce clamps

Given the options and technologies available in today's market, it is quite difficult to define the right technology and associated material. In this case, however, the priority is directed towards achieving the best possible mechanical properties. This is why FDM technology and a 3D printer from the company Markforged, specifically the X7 model, were chosen. Markforged is one of the few manufacturers

that offers high-quality composite materials capable of withstanding deployment in an industrial environment. Therefore, ONYX material with composite carbon fiber was used.

Tables 1 and 2 show the mechanical properties of the base material and composite fiber. Compared to other 3D printing technologies, which predominantly offer printing of the base material only, this technology stands out in terms of mechanical properties. FDM technology uniquely combines the relatively low cost of printing with high material strength.

Tab. 1: Mechanical properties of basic material [21].

Composite Base	Onyx
Tensile Modulus (GPa)	2.4
Tensile Stress at Yield (MPa)	40
Tensile Stress at Break (MPa)	37
Tensile Strain at Break (%)	25
Flexural Strength (MPa)	71
Flexural Modulus (GPa)	3.0
Heat Deflection Temp (°C)	145
Flame Resistance	-
Izod Impact - notched (J/m)	330
Surface Resistance (Ω)	-
Density (g/cm <sup>3</sup> )	1.2

Tab. 2: Mechanical properties – composite fiber [21].

Composite Base	Carbon
Tensile Strength (MPa)	800
Tensile Modulus (GPa)	60
Tensile Strain at Break (%)	1.5
Flexural Strength (MPa)	540
Flexural Modulus (GPa)	51
Flexural Strain at Break (%)	1.2
Compressive Strength (MPa)	420
Compressive Modulus (GPa)	62
Compressive Strain at Break (%)	0.7
Heat Deflection Temp (°C)	105
Izod Impact - notched (J/m)	960
Density (g/cm <sup>3</sup> )	1.4

Tab. 3: 3D printing parameters of CF/onyx profiles

Dimensions	65.9 x 95.0 x 35.0 mm
Printing Temperature (onyx)	274 °C
Printing Temperature (CF)	252 °C
Layer height	0.125 mm
Number of layers	264
Fiber Fill Type	Isotropic Fiber
Fill Pattern	Stripes
Fill Density	55%
Roof and Floor layers	2
Wall Layers	2

Print time	13 h a 17 min
Plastic Volume	70.73 cm <sup>3</sup>
Fiber Volume	11.71 cm <sup>3</sup>
Final Part Mass	72.6 g
Plastic Angles	0°, 45°, 90°, 135°
Fiber Angles	0°, 45°, 90°, 135°
Material cost	51.92 USD

### 2.2.2 Measurement of cutting forces

The principle of the entire test was to clamp the aluminum end-shield and simulate its machining with detailed capture of all data. A total of five were carried out, always with the new endshield, which then had to be systematically processed in the DynoWare software. Original steel clamps, an aluminum shield of the electric motor (see chapter 2.1.3) and a smooth-narrow machining knife were used for the test.

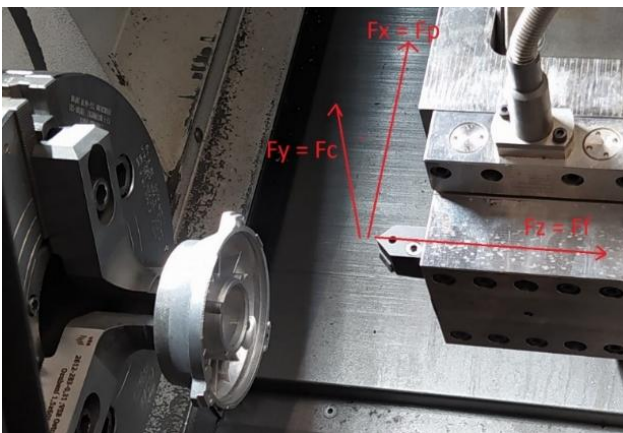


Fig. 8: Application of cutting forces on an experimental test.

### 2.2.3 Clamp finalization and testing

Before testing the clamps, it was necessary to perform post-processing in the form of setting the clamping stones (Fig. 9). These stones are universal and are therefore a purchased part. The minimum pressure for attaching an aluminum part is 8 bar.

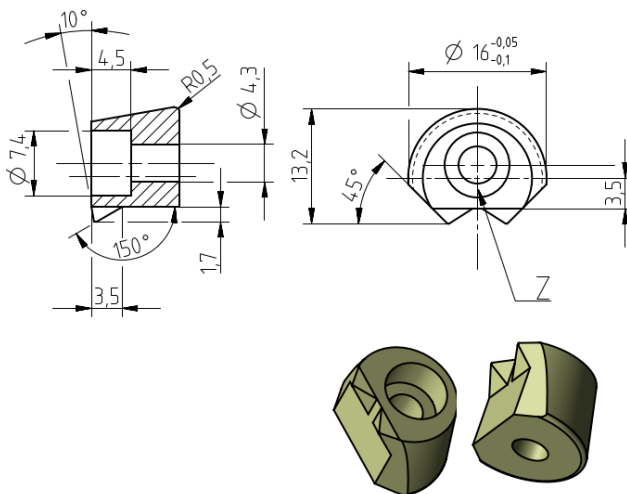


Fig. 9 – Sketch of a clamping stone.

## 3 EXPERIMENT AND RESULTS

### 3.1 Measurement results of measured data

After exporting all necessary measurements in \*.csv format, it was possible to examine all tens of thousands of measured values and select the largest measured data. These results were recorded in the simple table below. All data are necessary for the correct simulation of the clamp under the load of cutting forces.

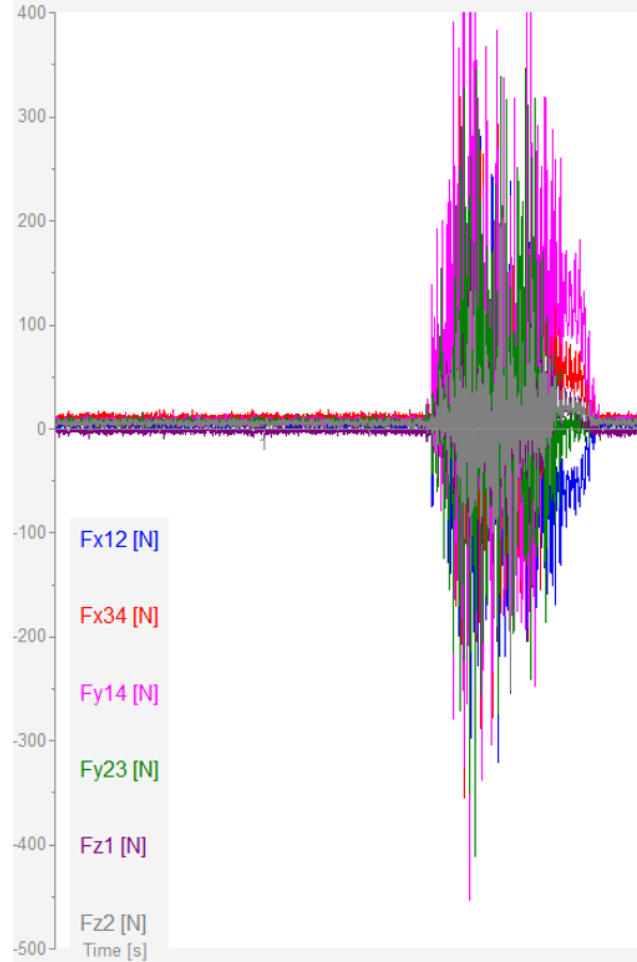


Fig. 10: Recording of measured forces in DynoWare software.

Tab. 4: Measured and evaluated maximum measured values.

No.	$v_c$	$f$	$F_x=F_p$	$F_y=F_c$	$F_z=F_f$
[-]	[m/min]	[mm]	[N]	[N]	[N]
1	785	0.3	199.28	589.91	228.27
2	785	0.3	239.87	574.34	230.10
3	785	0.3	199.89	612.18	206.60
4	785	0.3	230.41	616.76	182.80
5	785	0.3	232.85	697.94	182.80

Measurement of the resulting cutting force for the first to fifth measurements:

$$F = \sqrt{F_c^2 + F_p^2 + F_f^2} = \sqrt{F_x^2 + F_y^2 + F_z^2} \quad (1)$$

For the first measurement:

$$F_1 = \sqrt{199.28^2 + 589.905^2 + 228.271^2} = 663.1803 \text{ N} \quad (2)$$



For the second measurement:

$$F_2 = \sqrt{239.868^2 + 574.341^2 + 230.103^2} = 663.5900 \text{ N} \quad (3)$$

For the third measurement:

$$F_3 = \sqrt{199.89^2 + 612.183^2 + 206.604^2} = 676.3204 \text{ N} \quad (4)$$

For the fourth measurement:

$$F_4 = \sqrt{230.408^2 + 616.76^2 + 182.8^2} = 683.2983 \text{ N} \quad (5)$$

For the fifth measurement:

$$F_5 = \sqrt{232.849^2 + 697.937^2 + 182.8^2} = 758.1230 \text{ N} \quad (6)$$

The measured forces are therefore the limiting forces that arise during the machining of the aluminum shield. The values were measured on metal clamps to make the measurement accurate and informative.

After a mutual evaluation of the measured values with the catalog values of the chuck, the maximum forces in the individual axes at a speed of 2500 rpm were determined.

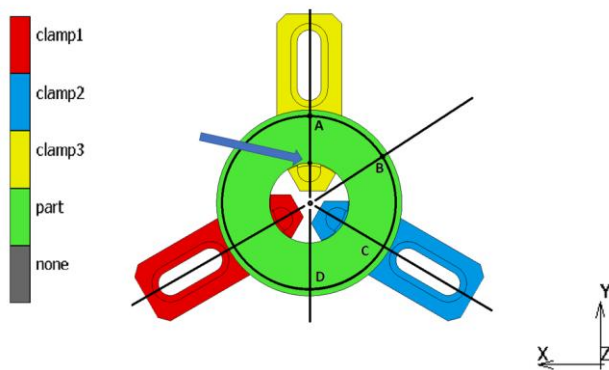


Fig. 11: Representation of the rotation system and division into planes.

The part is symmetrical. So, we can divide the part by symmetrical planes. A force can then be applied to A and The simulation was carried out in the Stress Analysis add-on of the Autodesk Inventor Professional 2024 application. The fixation was applied to the surface of the screw and the cutting force was applied to the Z position with the vector:

$$F = (233; 61; 78) \text{ N} \quad (12)$$

The geometry was meshed with 232203 elements and 338282 nodes. The result shows that the maximum Von Mises stress is 31.25 MPa, which gives a minimum factor of safety of 1.28 on the bolt surface.

### 3.2 Design of clamps printing

The clamp has been designed to minimize possible breakage or other deformation. Below in the picture is a projection of the use of composite fibers in connection with the base material. The entire design and correct layout of the fibers were based on accumulated experience [22]. The main emphasis was placed on the correct layout of the fibers to prevent breakage and minimize further deformations.

B. The maximum power at 2500 rpm after conversion to the simulation coordinate system is as follows:

$$F_x = 233 \text{ N} \quad (7)$$

$$F_y = 61 \text{ N} \quad (8)$$

$$F_z = 78 \text{ N} \quad (9)$$

$$F = \sqrt{F_x^2 + F_y^2 + F_z^2} \quad (10)$$

So, after substituting into the formula, the resulting force is:

$$F = \sqrt{233^2 + 61^2 + 78^2} = 253.17 \text{ N} \quad (11)$$

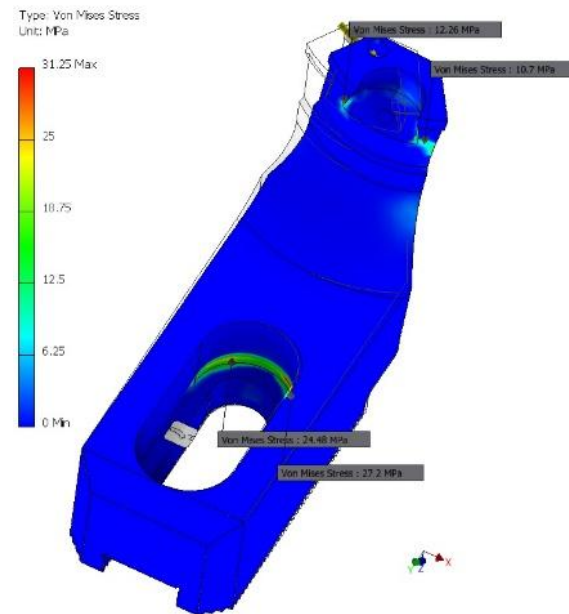


Fig. 12: Von Mises stress result.

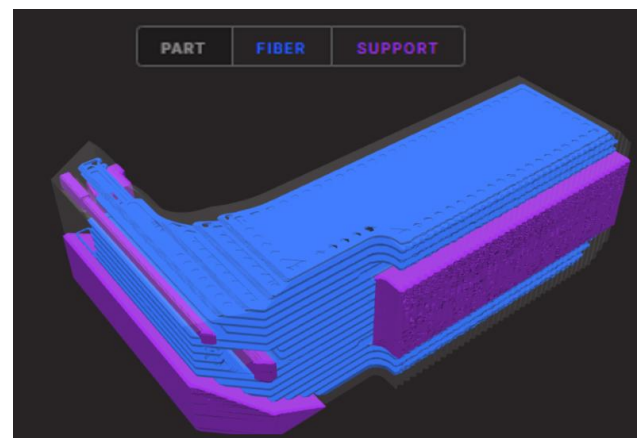


Fig. 13: Clamp design in SW from Markforged - ISO view.

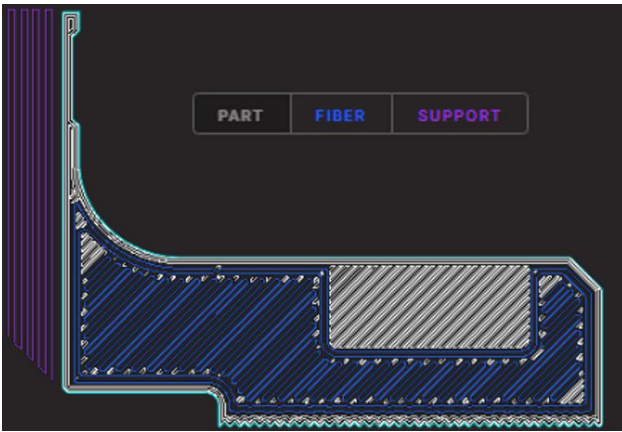


Fig. 14: Clamp design in SW by Markforged - side cut.

### 3.3 Testing the internal clamp

As part of the testing, the internal clamp was combined with the workpiece. The purpose of the clamp is to secure the part by the inner diameter. It is simpler to design and manufacture, but the clamping pressures act very strongly on the frame of the entire clamp. The clamp was made of ONYX material with carbon fiber.



Fig. 15: Chuck with internal clamps.



Fig. 16: Clamps before clamping the part.

During the first test of setting the clamping pressure to 10 bar, however, the aluminum part was not held by the clamps, and thus it was released into the machine space.

The following test was therefore set to a minimum value of 8 bar. At this value, the workpiece was maintained during the free rotation of the machine at low speeds, but when the machining knife and the workpiece met each other, it was released again into the machine space.

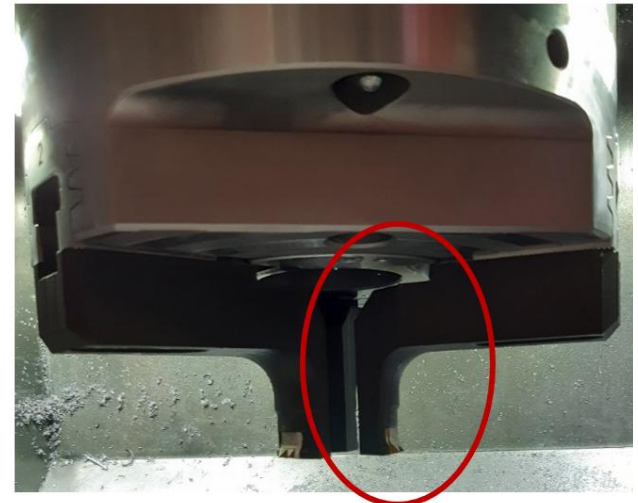


Fig. 17: Clamp without deformation (without load).

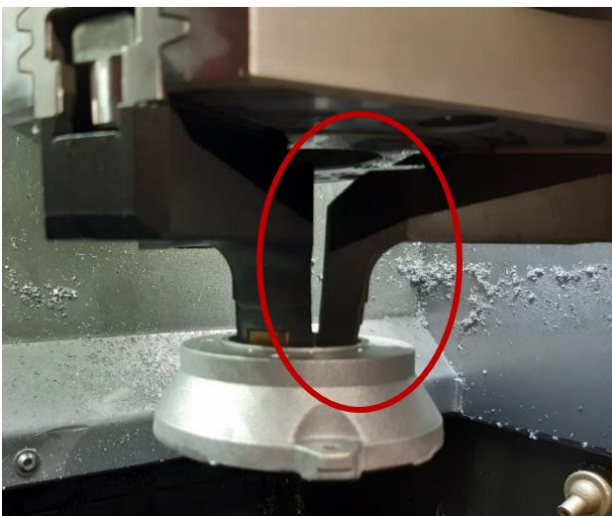


Fig. 18: Clamp with deformation (with load).

When examining the cause of this problem in detail, the deformation of the neck of the entire clamp was clearly visible. The conclusion was that even though it is a very strong plastic material (ONYX with carbon fiber), which according to its mechanical properties has relatively low elasticity, this assumption was completely wrong under load. The material is still very flexible for this type of application and in conjunction with this clamp design cannot compete with metal materials.

## 4 DISCUSSION

Unfortunately, the entire experiment with clamps made of a composite of plastic and special fibers turned out to be unsatisfactory for practical implementation in industrial use. The internal clamp was not strong enough to withstand the stress and therefore buckled. Although it returned to its original position after releasing the pressure, the clamp was unusable in industrial conditions.

However, this result has opened up other possibilities that can be explored and further developed. The future development of the idea of using a clamp made by 3D

printing will continue only with the combination of metal and topological optimization of the entire design. Satisfactory results cannot be achieved by simply replacing metal with plastic and its composites. Although the plastic material in combination with composite fibers is very strong, it still cannot compete with metal materials and is therefore not suitable for industrial use.

Within the framework of using FDM 3D printing technology in conjunction with composite materials [16] and ONYX material [15], there are recommended procedures for part design, implementation of composite fibers [17], and manufacturing parameters to achieve the highest possible mechanical properties.

As mentioned in the introduction, the idea of transferring a laboratory solution with clamps made of plastic composite to an industrial environment, with the help of current 3D printing technologies, is still insufficient. If we focus specifically on the printing of clamps, it is currently only used in medicine [23] in conjunction with 3D printing.

## 5 SUMMARY

The clamp experiment produced the following main findings:

- the clamps did not withstand strong clamping pressures and there was a deflection in the weakest point
- therefore, it was not possible to stably clamp and machine the part
- the calculation results were confirmed by experiment

Other positive findings:

- post-processing in the form of drilling is feasible for composite material
- the production accuracy of FDM technology is sufficient for preform production

Other negative findings:

- plastic materials and their special composites are not strong enough for use in heavy industrial environments

## 6 ACKNOWLEDGMENTS

A thank Mr. Ing. Petr Nemecek, Mr. Ing. Jiri Hajnys, Ph.D., Mr. Ing. Jakub Mesicek, Ph.D. and Mr. Ing. Antonin Trefil, Ph.D., who greatly contributed to the design, production and testing of clamps. I also thank them for their expert advice and mentoring, without these the article could not have been created.

Last, but not least, I would like to thank Mr. prof. Ing. Robert Cep, Ph.D., Mrs. prof. Ing. et Ing. Mgr. Jana Petru, Ph.D. and Mr. doc. Ing. Marek Pagac, Ph.D., who also contributed valuable advice, suggestions and experience, without which the article could not have reached the necessary quality.

This study was conducted in association with the project Innovative and Additive Manufacturing Technology - New Technological Solutions for 3D Printing of Metals and Composite Materials (reg. no. [CZ.02.1.01/0.0/0.0/17\\_049/0008407](https://doi.org/10.1016/j.049/0008407)) financed by Structural Funds of the European Union. *Article has been done in connection with project Students Grant Competition SP2024/087 „Specific Research of Sustainable Manufacturing Technologies“ financed by the Ministry of Education, Youth and Sports and Faculty of Mechanical Engineering VŠB-TUO.*

## 7 REFERENCES

- [1] [Sotola 2021] Sotola, M., Marsalek, P., Rybansky, D., Fusek, M., Gabriel, D., Sensitivity Analysis of Key Formulations of Topology Optimization on an Example of Cantilever Bending Beam, 2021, 13, <https://doi.org/10.3390/sym13040712>
- [2] [Mesicek 2021] Mesicek, J., Jancar, L., Quoc-Phu Ma, Hajnys, J., Tanski, T., Krpec, P., Pagac, M., Comprehensive View of Topological Optimization Scooter Frame Design and Manufacturing, 2021, 13, <https://doi.org/10.3390/sym13071201>
- [3] [Meng 2023] Meng, M., Wang, J., Huan, H., Liu, X., Zhang, J., Li, Z., 3D printing metal implants in orthopedic surgery: Methods, applications and future prospects, 2023, 94-112, ISSN 2214-031X <https://doi.org/10.1016/j.jot.2023.08.004>
- [4] [Long 2020] Long, Ch., Yanlai, Z., Zuyong, Ch., Jun, X., Jianghao, W. Topology optimization in lightweight design of a 3D-printed flapping-wing micro aerial vehicle, 2020, 3206-3219, ISSN 1000-9361, <https://doi.org/10.1016/j.cja.2020.04.013>
- [5] [Nickels 2014] Nickels, L., 3D printing the world's first metal bicycle frame, 2014, 38-40, ISSN 0026-0657 [https://doi.org/10.1016/S0026-0657\(14\)70083-9](https://doi.org/10.1016/S0026-0657(14)70083-9)
- [6] [Pianca 2022] Pianca, D., Carboni, M., Meyer, D., 3D-Printing of porous materials: Application to Metal-Organic Frameworks, 13, ISSN 2590-1508 <https://doi.org/10.1016/j.mtblux.2022.100121>
- [7] [Marsalek 2021] Marsalek, P., Sotola, M., Rybansky, D., Repa, V., Halama, R., Fusek, M., Prokop, J., Modeling and Testing of Flexible Structures with Selected Planar Patterns Used in Biomedical Applications, 2021, 14, <https://doi.org/10.3390/ma14010140>
- [8] [Gao 2015] Gao, W., Zhang, Y., Ramanujan, D., Ramani, K., Chen, Y., Williams, Ch. B., Wang, Ch. C. L., Shin, Y. C., Zhang, S., Zavattieri, P. D., The status, challenges, and future of additive manufacturing in engineering, 2015, 65-89, ISSN 0010-4485 <https://doi.org/10.1016/j.cad.2015.04.001>
- [9] [Graf 2023] Graf, S., Thakkar, D., Hansa, I., Pandian, S. M., Adel, S. M., 3D Metal Printing in Orthodontics: Current Trends, Biomaterials, Workflows and Clinical Implications, 2023, 34-42, <https://doi.org/10.1053/j.sodo.2023.01.001>
- [10] [Buchanan 2019] Buchanan, C., Gardner, L., Metal 3D printing in construction: A review of methods, research, applications, opportunities and challenges, 2019, 332-348, ISSN 0141-0296 <https://doi.org/10.1016/j.engstruct.2018.11.045>
- [11] [Wu 2016] Wu, P., Wang, J., Wang, X., A critical review of the use of 3-D printing in the construction industry, 2016, 21-31, ISSN 0926-5805 <https://doi.org/10.1016/j.autcon.2016.04.005>
- [12] [Cesaretti 2014] Cesaretti, G., Dini, E., Kestelier, D. X., Colla, V., Pambaguian, L., Building components for an outpost on the Lunar soil by means of a novel 3D printing technology, 2014, 430-450, ISSN 0094-5765 <https://doi.org/10.1016/j.actastro.2013.07.034>
- [13] [Hager 2016] Hager, I., Golonka, A., Putanowicz, R., 3D Printing of Buildings and Building Components as the Future of Sustainable



- Construction?, 2016, 292-299, ISSN 1877-7058  
<https://doi.org/10.1016/j.proeng.2016.07.357>
- [14] [Sama 2019] Sama, S. R., Badamo, T., Lynch, P., Manogharan, G., Novel sprue designs in metal casting via 3D sand-printing, 2019, 563-578, ISSN 2214-8604  
<https://doi.org/10.1016/j.addma.2018.12.009>
- [15] [Bianco 2020] Blanco, I., The Use of Composite Materials in 3D Printing, 2020, 22,  
<https://doi.org/10.3390/jcs4020042>
- [16] [Kalova 2021] Kalova, M., Rusnakova, S., Krzikalla, D., Mesicek, J., Tomasek, R., Podeprelova, A., Rosicky, J., Pagac, M., 3D Printed Hollow Off-Axis Profiles Based on Carbon Fiber-Reinforced Polymers: Mechanical Testing and Finite Element Method Analysis, 2021, 17,  
<https://doi.org/10.3390/polym13172949>
- [17] [Li 2025] Li, S., Zhang, H., Lu, Z., Cao, F., Wang, Z., Liu, Y., Zhu, X., Ning, S., Miao, K., Qiu, S., Li, D., Fabrication of bamboo-inspired continuous carbon fiber-reinforced SiC composites via dual-material thermally assisted extrusion-based 3D printing, 2025, 92-103, ISSN 1005-0302  
<https://doi.org/10.1016/j.jmst.2024.04.048>
- [18] [Vedrtnam 2023] Vedrtnam, A., Ghabezi, P., Gunwant, Dheeraj., Jiang, Y., Sam-Daliri, O., Harrison, N., Goggins, J., Finnegan, W., Mechanical performance of 3D-printed continuous fibre Onyx composites for drone applications: An experimental and numerical analysis, 2023, 12, ISSN 2666-6820  
<https://doi.org/10.1016/j.jcomc.2023.100418>
- [19] [Petcharat 2023] Petcharat, N., Wiangkham, A., Pichitkul, A., Tantrairatn, S., Aengchuan, P., Bureerat, P., Banpap, S., Khunthongplatprasert, P., Ariyarat, A., The multi-objective optimization of material properties of 3D print onyx/carbon fiber composites via surrogate model, 2023, 37, ISSN 2352-4928  
<https://doi.org/10.1016/j.mtcomm.2023.107362>
- [20] [Ramalingam 2021] Ramalingam, P. S., Mayandi, K., Balasubramanian, V., Chandrasekar, K., Stalany, V. M., Munaf, A. A., Effect of 3D printing process parameters on the impact strength of onyx – Glass fiber reinforced composites, 2021, 6154-6159, ISSN 2214-7853  
<https://doi.org/10.1016/j.matpr.2020.10.467>
- [21] [Markforged 2024] MARKFORGED, 3D Printing Materials, online. 2024.  
<https://markforged.com/materials>. [cit. 2024-07-01].
- [22] [Krzikalla 2022] Krzikalla, D., Mesicek, J., Halama, R., Hajnys, J., Pagac, M., Cegan, T., Petru, J., On flexural properties of additive manufactured composites: Experimental, and numerical study, 2022, 11, ISSN 0266-3538  
<https://doi.org/10.1016/j.compscitech.2021.109182>
- [23] [Cornaz 2021] Cornaz, F., Burkhard, M., Fasser, M. R., Spirig, J. M., Snedeker, J. G., Farshad M., Widmer, J., 3D printed clamps for fixation of spinal segments in biomechanical testing, Journal of Biomechanics, 2021, 125, ISSN 0021-9290,  
<https://doi.org/10.1016/j.jbiomech.2021.110577>